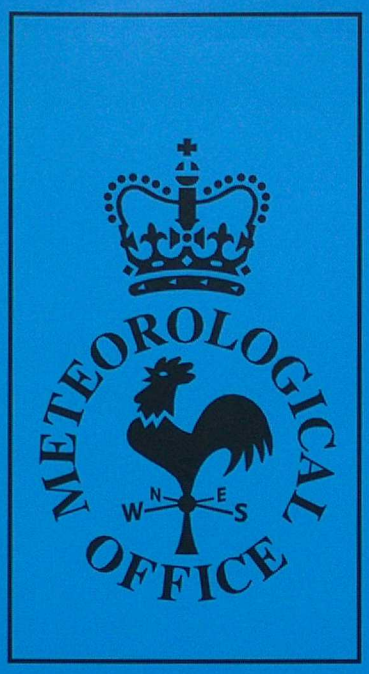

Forecasting Research

Forecasting Research Division
Technical Report No. 9

Spin up problems of the UKMO mesoscale model and moisture nudging experiments

by

Akihide Segami

February 1992

Meteorological Office
London Road
Bracknell
Berkshire
RG12 2SZ
United Kingdom

Short-Range Forecasting Research Division

TECHNICAL REPORT NO 9

Spin up problems of the UKMO mesoscale model and moisture nudging experiments

by

Akihide Segami

(*Japan Meteorological Agency*)

February 1992

Short-Range Forecasting Research Division,
Meteorological Office,
London Road,
Bracknell,
Berkshire,
RG12 2SZ,
United Kingdom.

ABSTRACT

Spin up problems of the UKMO mesoscale model are investigated. Most of the spin up problems in the model come from the initial dynamical imbalance between the mass and wind fields. Large surface pressure oscillations and large vertical motion are generated in the model. This imbalance, linked with the precipitation process, produces spurious stratiform rainfall during the first stage of the forecast.

The convection scheme also gives rise to serious problems. Spurious oscillatory behaviour of the convective rain rate appears at the beginning. A more serious problem is that the convection scheme does not work well and most of the rainfall comes from the stratiform cloud scheme even in a very unstable situation. It is necessary to re-examine both the convective and stratiform cloud schemes.

In order to reduce the spin up problem and to use high resolution moisture data, a so called nudging technique is adopted in the mesoscale model. The model fields are nudged toward IMI (Interactive Mesoscale Initialization) produced relative humidity and liquid water mixing ratio fields. This moisture nudging is effective to reduce the spin up problem. The method also has an impact on the precipitation forecasts in both convective and frontal cases for the first several hours. However, the impact becomes marginal after that. The results may depend not only on the synoptic situation but also on the model's forecast domain and physical parameterization schemes.

1. Introduction

The performance of numerical weather prediction models has been significantly improved recently, and reliable forecasts for large-scale disturbances can be obtained for up to three or four days. However, good prediction of the large-scale disturbances does not always lead to an accurate weather forecast. Mesoscale phenomena such as mesoscale convective systems and severe rainstorms in frontal systems must be predicted precisely. For this purpose, several numerical weather prediction centres have developed so called mesoscale models operationally; for example, the Japan Spectral Model in the Japan Meteorological Agency (Segami et al., 1989) and the UKMO mesoscale model (Golding, 1990).

One of the important targets of the mesoscale models is a very short-range forecast. An objective nowcasting system for precipitation forecasts has been introduced operationally in the Japan Meteorological Agency since April 1988. Because the method is linear extrapolation of the past movement of echoes and no development or decay of them is considered in the model, the skill decreases rapidly until three hours, although it still exceeds that of persistence forecasts. For predictions beyond three hours, it is necessary to use numerical prediction models which can treat non-linear effects.

However, there are significant problems to be solved in most of the mesoscale models in order to use them for very short-range forecasts. There is often a spin up problem. A lot of mesoscale models suffer weak precipitation rates in the first few hours of the forecast (Segami et al., 1989 and DiMego et al., 1991, etc.). According to Segami et al., the major reason for slow spin up is that the analyzed or initial fields contain no appropriate mesoscale structures. To cope with this problem, Takano and Segami (1991) used high resolution radar and rain-gauge network data for moisture initialization and diabatic NNMI (Non-linear Normal Mode Initialization) in the Japan Spectral Model. They also adopted a forecast/analysis cycle in the model. They found the spin up problem to be completely resolved using the above methods.

The UKMO mesoscale model shows a quite different spin up problem from the Japan Spectral Model. The first objective of this paper is to describe the spin up problem and to clarify the reasons for the problem in the UKMO mesoscale model. Then, we introduce a so called nudging technique in the model to improve the spin up problem. Since high resolution moisture data are very important for mesoscale forecasts as shown by Takano and Segami(1991), we use relative humidity and liquid water fields produced from the IMI using radar and satellite data and we investigate the effects of the nudging for convective and frontal cases.

2. Spin up problem in the UKMO mesoscale model

Because predicting a severe rainstorm is one of the most important objectives of a mesoscale model, we choose a severe thunderstorm case to investigate spin up problems of the UKMO mesoscale model. Figure 1 shows convective precipitation areas from 00z to 12z on 6th July 1991 analysed from surface synoptic charts. The thunderstorm area located over the south coast of England at 00z moves gradually northward and reaches the north of England at 12z.

The initial time of the forecast is 00z July 6th. The initial fields are produced from the IMI. The model used in this experiment is basically the same as the operational mesoscale model. The model uses a non-hydrostatic formulation for its dynamical framework with horizontal resolution of 15km and 32 vertical levels. The convection scheme is formulated based on the idea of Fritsch and Chappell (1980). For more details, see Golding (1990).

Figure 2 shows the time evolution of convective and stratiform precipitation rates and the total sum of them averaged over the forecast domain (the outermost two grid points are excluded in the average). The values are plotted every 15 timesteps starting from the 15th step because convective cells are produced at these timesteps (Δt=1 min.). Two typical spin-up problems can be seen. One is a spurious oscillatory behaviour of the convective rainfall rate and the other is an enormous amount of stratiform rainfall at the beginning of the forecast.

The behaviour of the convective rain is related to the number of convective cells created in the model (Figure 3). Initially, the first time the convection scheme is called, a lot of convective clouds are created in an unstable atmospheric situation. Because the life time of each convective cell is prescribed as just one hour, the clouds created at first disappear after one hour. The convection scheme needs several atmospheric conditions to be satisfied in order to generate a convective cell (Barnes and Golding, 1986). In nature, the life time depends on the atmospheric conditions and cells are created one after another to respond large scale forcing. However it appears in the model that after a large number of convective cells have been created in response to the initial unstable profiles, the atmospheric conditions then become unfavourable to the production of further convective cells. The total number of cells reduces significantly after one hour when the initial cells have died out. There is a delay in the production of a significant number of convective cells until the required conditions ('trigger mechanisms') for convection are produced by the large scale forcing. The reason for this behaviour needs further investigation. It is possible that the convection scheme may itself be reducing the production of convection. However, it may also be due to larger scale responses to imbalances in the mass, wind and humidity fields as will be mentioned below.

Concerning the stratiform rain, while a lot of other mesoscale models suffer too weak rainfall for the first few hours, the UKMO mesoscale model shows the opposite spin up problem. The major production terms of precipitation in the stratiform cloud scheme are accretion and melting. As shown in Figure 4, the accretion term is the main reason for this spin up problem. The accretion term in the model can be written as

follows:

$$ACC \propto m \cdot Pr$$

where m and Pr denote cloud water and precipitation rate, respectively. Because precipitation rate is also proportional to cloud water (or cloud ice), the accretion term quite effectively converts cloud water to rain where a lot of cloud water exists. Within one hour, most of the cloud water falls out (Figure 5) and the precipitation due to accretion rapidly decreases. On the other hand, cloud ice increases gradually and the melting of snow or cloud ice (there is no difference between snow and cloud ice in the model) becomes the major production term.

To clarify the above mentioned process, we select the point (Point A hereafter) where highest precipitation rate is predicted. Figure 6 shows the vertical distribution of rain rates and snow rates in the stratiform cloud scheme at timesteps 15 and 120. Production of rain due to accretion is also depicted. At timestep 15, snow is gradually produced at levels 30 to 24 and the rate just above freezing level becomes about 10 mm/h. It is converted to rain instantaneously at level 23. Below the freezing level, rain is created rapidly due to accretion and the rain rate reaches almost 90 mm/h near the surface. At timestep 120 most of the cloud water falls out and the major part of the liquid water content becomes cloud ice. The accretion effect becomes small and the major part of the rain comes from melting of snow.

Figure 7 shows another serious problem. Too much liquid water is accumulated in the upper troposphere. The value of 4~5 g/kg at the 27th level is more than twice that of the saturation humidity mixing ratio at that level. To investigate the reason for this, we plotted the time sequence of vertical velocity, liquid water mixing ratio and surface pressure at Point A. Precipitation rates are also plotted. Spurious oscillation of the surface pressure and an extraordinarily large amount of vertical motion (~18m/s) are produced within the first 20 timesteps. This vertical motion advects total water upward and accumulates too much liquid water (~7g/kg), which produces enormous stratiform rainfall (~120mm/h). Almost the same amplitude of surface pressure oscillation and vertical motion are predicted by a dry model whose convection scheme and stratiform cloud scheme are switched off. This indicates the existence of initial dynamical imbalance between the mass and momentum fields.

The above mentioned process which leads to spurious rainfall in the mesoscale model can be summarized as follows:

(a) Initial imbalance between the wind and mass fields produces spurious oscillation in the surface pressure and an enormous amount of vertical motion.
(b) The extraordinary vertical motion advects too much total water upwards, which is accumulated in the middle or upper troposphere as liquid water (cloud water or cloud ice). The accumulated liquid water mixing ratio reaches a value two or three times larger than the saturation humidity mixing ratio at each level.
(c) Large amounts of cloud water can produce enormous amounts of rainfall through the accretion process in the model.
(d) Within one hour, most of the cloud water below freezing level falls out as rainfall because of the quite effective accretion process. From then, the dominant contribution to rainfall becomes the melting of snow.

(e) The process (c) and (d) entirely stabilizes the atmosphere in just one hour (Figure 9).

The model also has problems related to the convection scheme. The spurious oscillation of the rainfall rate is highly connected with the prescribed life time of convective cloud cells. The other significant problem is that the model produces rainfall mostly through the stratiform cloud, not convective cloud, even in an unstable situation. The stratiform cloud scheme release convective instability after the enormous amount of liquid water is accumulated in the middle and upper troposphere, while the convection scheme does not work well.

3. Moisture nudging in the mesoscale model

Most of the spin-up problems, except in the convective rainfall, come from the initial imbalance of the model atmosphere. In order to reduce spurious gravitational oscillation, a lot of numerical models adopt the nonlinear normal mode initialization (NNMI) technique. However, the method has not been established in a non-hydrostatic model which includes not only gravity waves but also sound waves. One may reduce the oscillation due to gravity waves by applying NNMI to a hydrostatic model with the same resolution, same vertical levels and same orography as the non-hydrostatic model. However, besides the problem of sound waves, the validity of NNMI which assumes zero tendency for gravity waves becomes uncertain for a high resolution model. Moreover, the NWP system should be more flexible for new types of observations such as from aircraft or remote sensing.

In this context, we are going to adopt a nudging technique in the mesoscale model. The method has been successfully introduced in the UKMO global and limited area systems since 1982 (Bell and Dickinson (1987); Lorenc et al.(1991)). According to Lorenc (1991, personal communication), spin up problems are completely resolved in the global model, at least in a global mean sense.

Because high resolution moisture fields are very important in mesoscale forecasts, we use relative humidity and liquid water fields which are produced by the IMI from radar and satellite observations and investigate the impact of moisture nudging. The formulation of the assimilation is the same as Hoke and Anthes (1976). Since the forecast variables are total water ($q_t = q + q_L$) and liquid water potential temperature ($\theta_L = \theta - Lq_L/C_p\pi$), we use the following equations for the nudging experiment.

$$\partial q_t/\partial t = F(q_t) - G(t) \left(q_t - q^{*IMI} - q_L^{IMI} \right) \qquad (1)$$

$$\partial \theta_L/\partial t = F(\theta_L) + (L/C_p\pi)\, G(t) \left(q_L - q_L^{IMI} \right) \qquad (2)$$

$$q^{*IMI} = R_H^{IMI} q_s(T)$$

where, q_L^{IMI} and R_H^{IMI} are IMI-produced liquid water mixing ratio and relative humidity, respectively, $q_s(T)$ is the saturation humidity mixing ratio and G(t) a nudging coefficient depending on time as shown in Figure 10. In this figure, -ts and te are the start and end times of the nudging, respectively. To see the impact of the nudging, we carried out the following four types of experiments (see Figure 11) :

IMIF : normal forecast starting from T+0 IMI.

NUGE : nudging experiment starting from T-3 interpolated limited area model fields (LAM).
ts = 3 hours, te = 1 hour,
G_0 = 2.0/ts = 1.0 / 1.5 (1/hour)

NONG : experiment without nudging initiated from the same field as NUGE experiment.

DNGE : nudging experiment with a delta function type nudging coefficient.
ts = te = Δt = 1 min.
G_0 = 2.0/ts = 2.0/60 (1/sec)

DNGE corresponds to the experiment where the moisture field is instantaniously replaced by the IMI at T+0 in the NONG experiment. We start the assimilation from T-3. For the start field, we use an interpolated limited area model forecast instead of the previous IMI at T-3. As described in Section 2, the model forecast initiated from the IMI suffers serious dynamical imbalance which may change the atmospheric conditions significantly through diabatic processes before balanced fields are obtained.

==========

Footnote :
Without the model forcing, eqs. (1) and (2) can be written as follows.

$$\partial X/\partial t = - G(t) (X-Xa),$$

where Xa means the analyzed field of X at t=0. The equation can be solved analytically and the value of X at t=0 becomes

$$X(t=0) = Xa \{ 1-\exp(-G_0 ts/2) \} = 0.632\ Xa,$$

where

$$G_0 ts/2 = 1$$

is used.

4. Results of nudging experiments

We chose two cases to investigate the impact of the humidity nudging. One is the case mentioned in Section 2 and the other is a case of a warm front passage.

4.1 Severe rainfall accompanying thunderstorms (July 6th, 1991)

This is the case mentioned in Section 2. Figure 12 shows relative humidity from the IMI (analysis), NUGE, NONG and DNGE at 00z July 6th at the 1020m level. Impacts from the nudging in both the NUGE and DNGE experiments are obvious compared with NONG. The NUGE experiment nudges the field well towards IMI with some smoothing effects. DNGE retains more mesoscale features observed in IMI. These facts show that the nudging term works well in the model.

Figure 13 shows the present weather from IMIF, NUGE and NONG at T+1 and T+3. There is a typical spin-up problem in the IMIF experiment. The precipitation area appearing in IMIF at T+1 shrinks rapidly at T+3. The NUGE and NONG experiments have not such spin-up problem and the areas of precipitation do not change so much in these experiments. Compared with NONG, NUGE has a wide precipitation area, which agrees well with observations. Figure 14 depicts area averaged precipitation rates for NUGE, NONG and DNGE. Oscillatory behaviour of the convective rainfall is still present in these experiments. This feature seems unavoidable in the model so long as the model uses the convection scheme. These oscillations become weak after T+0 in the NUGE and NONG experiments, and then both convective and stratiform rain rates change smoothly with time. However, the DNGE experiment suffers another spurious oscillation after T+0, related to the convection scheme. This is because the rather spotty relative humidity field shown in Figure 12 re-generates a lot of convective cells.

The impact of moisture nudging shown in Figure 13 decreases gradually and the differences among IMIF, NUGE and NONG become marginal at T+9 (Figure 15). Most of the convective system has disappeared in the model although in reality the system persisted until 12z. We think the deficiency of the precipitation process in the model is the major reason. Figure 16 shows time sequences of precipitation rate, vertical velocity, liquid water mixing ratio and sea level pressure for the grid point (41,64) in the NUGE experiment. The initial imbalance is not very large, as shown in the surface pressure. However, almost the same things happen as in the IMIF experiment in Figure 8. The convective rain rate is quite weak and a lot of liquid water is accumulated in the upper atmosphere. Then severe rainfall comes from the stratiform cloud scheme with a vertical velocity of about 5 m/s. Moreover, the spurious pressure oscillation is observed around the time that the heavy rainfall happens. In order to maintain the mesoscale convective system, not only the large scale forcing but the heating profile of the convection itself is very important. In the model, the convective system can not persist longer because most of the diabatic heating comes from the stratiform cloud scheme which stabilizes the atmosphere rapidly.

4.2 Frontal case (October 30th 1991)

The previous case was not suitable to see the impact of data assimilation because of the weakness of the convection scheme. Hence we chose a rather weak rainfall case due to a warm front. Figure 17 shows the Meteosat infrared images at 06, 09 and 12z on October 30th 1991. A frontal system stretches from north to south and moves eastwards, gradually decreasing in strength. Figures 18 and 19 show the present weather charts at T+1 and T+3 of IMIF and NUGE respectively. IMIF has a similar spin up problem to that in the previous case, and the NUGE experiment reduces the problem. To see the impact of moisture nudging, we compare the forecast of NUGE with the NONG and DNGE experiments at T+3 (Figure 19). The width of the rain bands is rather different in these experiments although their positions are almost the same. NUGE has the widest band and NONG has the narrowest one. The width of the band can not be compared with the Meteosat images directly. Considering the time evolution, the band in NONG becomes wider from T+3 to T+6 (Figure 21) which does not agree with the Meteosat images, while in NUGE it persists with almost the same width. However, the differences between forecasts become negligible after 6 hours of assimilation as shown in Figure 21.

5. Concluding remarks

In this study, we investigated spin up problems in the UKMO mesoscale model and tested the effects of moisture nudging in the model. The formulation of the nudging is the same as Hoke and Anthes (1976) and the fields are nudged towards IMI-produced relative humidity and liquid water mixing ratio analyses.

Most of the spin up problems in the mesoscale model come from the initial dynamical imbalance between mass and wind fields. In the convective case, a surface pressure oscillation of amplitude 7 mb and vertical velocity of 18 m/s is generated in the first 20 timesteps. This value almost breaks the CFL condition in the vertical (Actually, the model blew up when initiated from the T-3 IMI because of the vertical CFL condition). This extraordinary vertical motion advects large amounts of total water upward and accumulates a lot of liquid water in the middle and upper troposphere. Then an enormous amount of stratiform rain is produced due to the accretion term of the model and the stability of the atmosphere is significantly changed in one or two hours.

The problem of the initial conditions which leads to many failures has already been pointed out by Ballard (1991). In the IMI, adjustments are made to the low level temperature and wind fields on the basis of surface analyses, and corrections are also made to temperature, wind and upper-level pressure fields in an attempt to ensure consistency with mean-sea-level pressure and cloud analyses (Wright and Golding, 1990). However, no dynamical balance is considered in terms of gravitational oscillations. Although some of the correction processes were removed from the IMI, there still exists a large imbalance. We think it is necessary to remove or improve most of the correction processes. Otherwise, use of the interpolated LAM field is much better as far as the initial imbalance is concerned.

Problems in the convection scheme are also serious. A spurious oscillatory behaviour of the convective rainfall rate is predicted for the first stage of the forecast. This is highly connected with the prescribed life time of the convective clouds. This problem may be reduced with the nudging process. The following problem is more serious. The model produces rainfall mostly through the stratiform cloud scheme, even in a very unstable situation. At 15km resolution, it is not clear whether a convective parameterization should be used because it is an intermediate scale between resolved and subgrid scale convection. In some frontal simulations, the convective parameterization is not needed (Ballard (1992), personal communication). However, the heating profiles infered from Figure 6 are very spurious compared with observations (for example from GATE data by Thompson et al., 1979). The amount of liquid water accumulated in the upper troposphere is enormously large. Moreover, the problem is that the heating profile acts to weaken the convective system, not to maintain it. It is necessary to re-examine both the convection scheme and the stratiform scheme and their interaction. The reason should be also examined for the high vertical velocity and pressure changes appearing in Figure 16 in the NUGE experiment.

The objectives of the nudging experiments were to reduce the spin up problem of the model whilst still using the high resolution moisture and cloud data derived from radar and satelite. The nudging experiment denoted NUGE is effective in reducing the problem, while the delta-function type nudging (DNGE) produces another oscillatory behaviour related to the convective scheme. The method also has a positive impact on the precipitation forecasts in both convective and frontal cases in the first several hours. However, the impact becomes marginal after that. For the frontal case, we think this is due to relatively strong large scale forcing and the small forecast domain compared with the disturbance. On the other hand, although the large scale forcing is weak and the disturbance is relatively small in the July case, the deficiency of the convection scheme limits the beneficial effects of the nudging. Much more impacts of the initial moisture fields were obtained in some experiments where large scale forcing is weak; for example in an anti-cyclonic stratiform cloud case by Bell and Hammon (1988) and in a sea fog case by Ballard et al.(1991). Generally speaking, the impact of moisture fields is large when large scale forcing is weak, especially when the moisture field plays a significant role for convective forcing (Takano and Segami, 1990). However, as mentioned above, the impact also depends on the model's forecast domain and its physical parameterization schemes. Further research is necessary for various synoptic situations to conclude this moisture nudging investigation.

Acknowledgments

I would like to thank the Japan Meteorological Agency and the United Kingdom Meteorological Office for giving me the opportunity for research in the UKMO. Financial support was given by the Japan Science and Technology Agency. I would also like to thank S. Ballard, B. Macpherson, R. Barnes and B. Wright for helping me to use the mesoscale model and the graphics system and for their useful discussion and comments.

References

Ballard, S.P., 1991: Assessment of the performance of the 32 level version of the mesoscale model. Short-range Forecasting Research, Tech. Note No. 62.

Ballard, S.P., 1991: Mesoscale model experimental forecasts of the haar of northeast Scotland., Mon. Wea. Rev., 119, 2107-2123.

Barnes, R.T.H. and B.W. Golding, 1986: A parameterization of deep convection for use in a non-hydrostatic mesoscale model, Met O 11 Tech. Note No. 229.

Bell, R.S. and A. Dickinson, 1987: The Meteorological Office operational numerical weather prediction system. Sci. Paper No.41, Meteorological Office.

Bell, R.S. and O. Hammon, 1988: The sensitivity of fine-mesh rainfall forecasts to changes in the initial moisture fields. Forecasting Research, Met O 11 Tech. Note No. 16.

DiMego, G.J., K.E. Mitchell, R.L. Wobus, R.A. Petersen, J.P. Gerrity, J.E. Hoke, and H-M. H. Juang, 1991: Pre-implementation testing of the NMC regional data assimilation system. Ninth AMS conference on numerical weather prediction, 221-224.

Fritsch, J.M. and C.F. Chappell, 1980: Numerical Prediction of Convectively Driven Mesoscale Pressure Systems. Part 1: Convective Parameterization. J. Atmos. Sci., 37,1722-1733.

Golding, B.W., 1990: The Meteorological Office mesoscale model. Meteor. Mag. 119, 81-96.

Hoke, J.E. and R.A. Anthes, 1976: The initialization of numerical models by a dynamic-initialization technique. Mon. Wea. Rev., 104, 1551-1556.

Lorenc, A.C., R.S. Bell and B. Macpherson, 1991: The Meteorological Office analysis correction data assimilation scheme., Q.J.R. Meteorol. Soc., 117, 59-89.

Segami, A., K. Kurihara, H. Nakamura, M. Ueno, I. Takano and Y. Tatsumi, 1989: Operational mesoscale weather prediction with Japan Spectral Model. J. Meteor. Soc. Japan, 67, 907-924.

Takano, I. and A. Segami, 1991: Improvement of the spin up problem with the Japan Spectral Model. Suuchiyohou-ka Houkoku Bessatsu, 37, 48-66, in Japanese.

Thompson, R.M., S.W. Payne, E.E. Recher and R.J. Reed, 1979 : Structure and properties of synoptic scale wave disturbances in the intertropical convergence zone of the Eastern Atlantic., J. Atmos. Sci., 36, 53-72.

Wright, B.J. and B.W. Golding, 1990: The Interactive Mesoscale Initialization. Meteor. Mag, 119, 234-244.

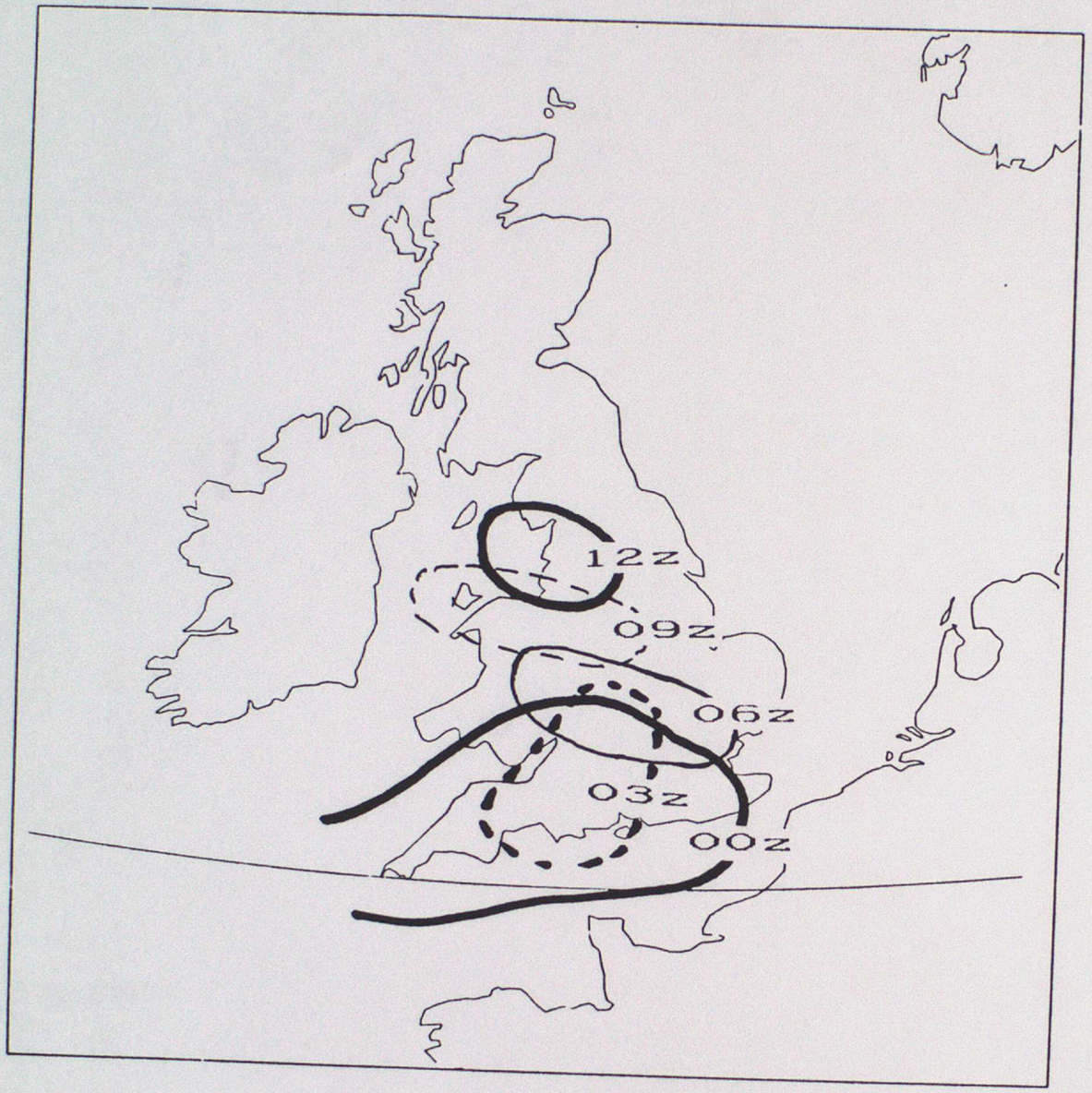

Figure 1 : Convective precipitation area from 00z to 12z on 6th July 1991 analysed from surface synoptic charts.

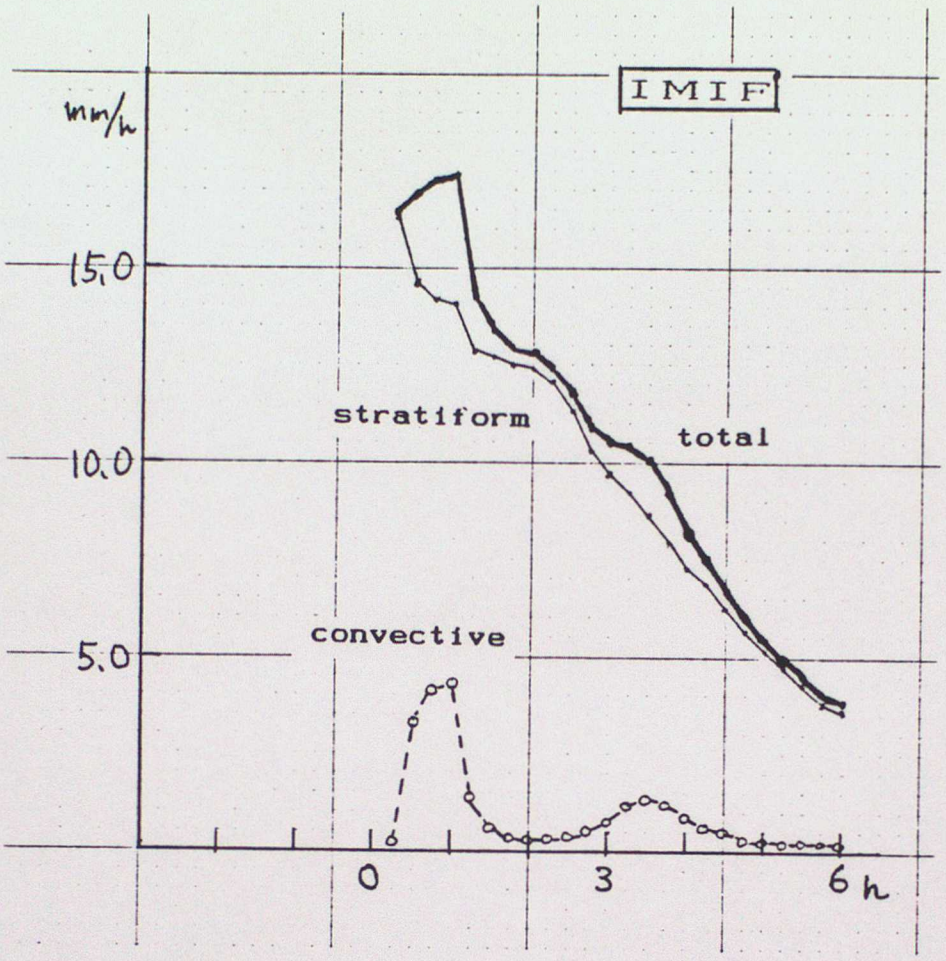

Figure 2 : Area averaged precipitation rate of stratiform rain, convective rain and the total sum of them. The values are plotted every 15 timesteps starting from the 15th step because convective cells are produced at these timesteps.

Figure 3 : Number of cloud cells created in the convection scheme.

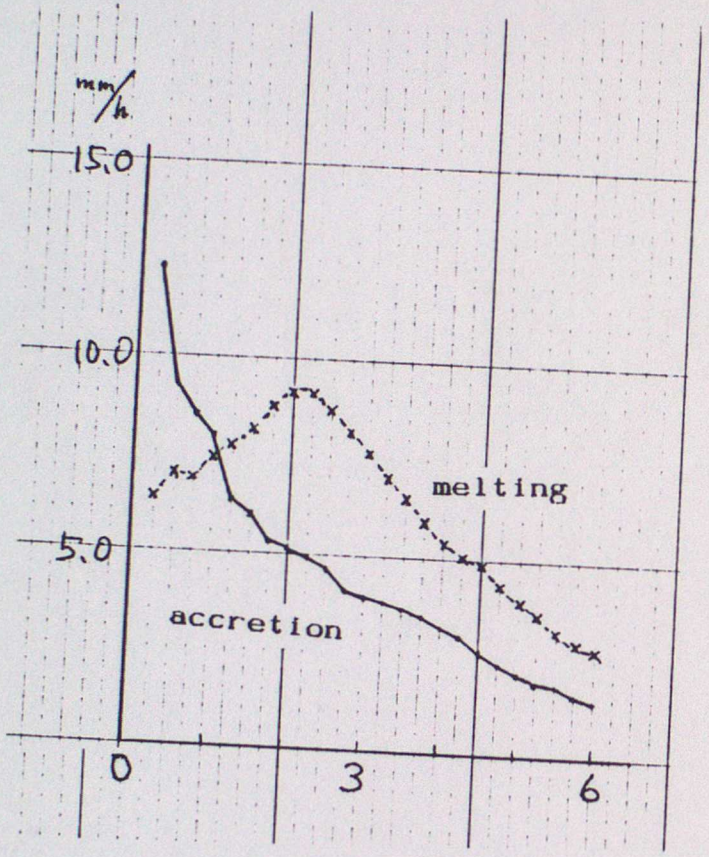

Figure 4 :

Production of stratiform rain due to accretion and melting in the model. The other explanations are the same as for Figure 2.

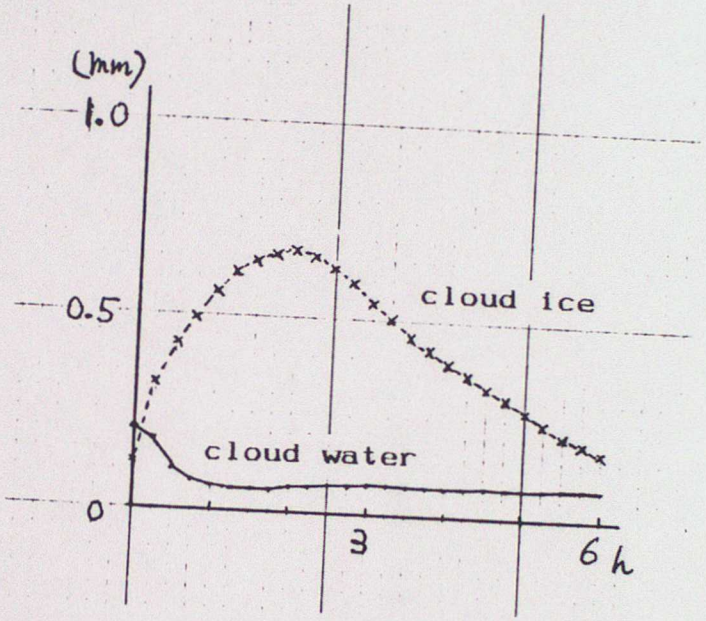

Figure 5 :

Cloud water and cloud ice contained in the atmosphere averaged over the forecast domain.

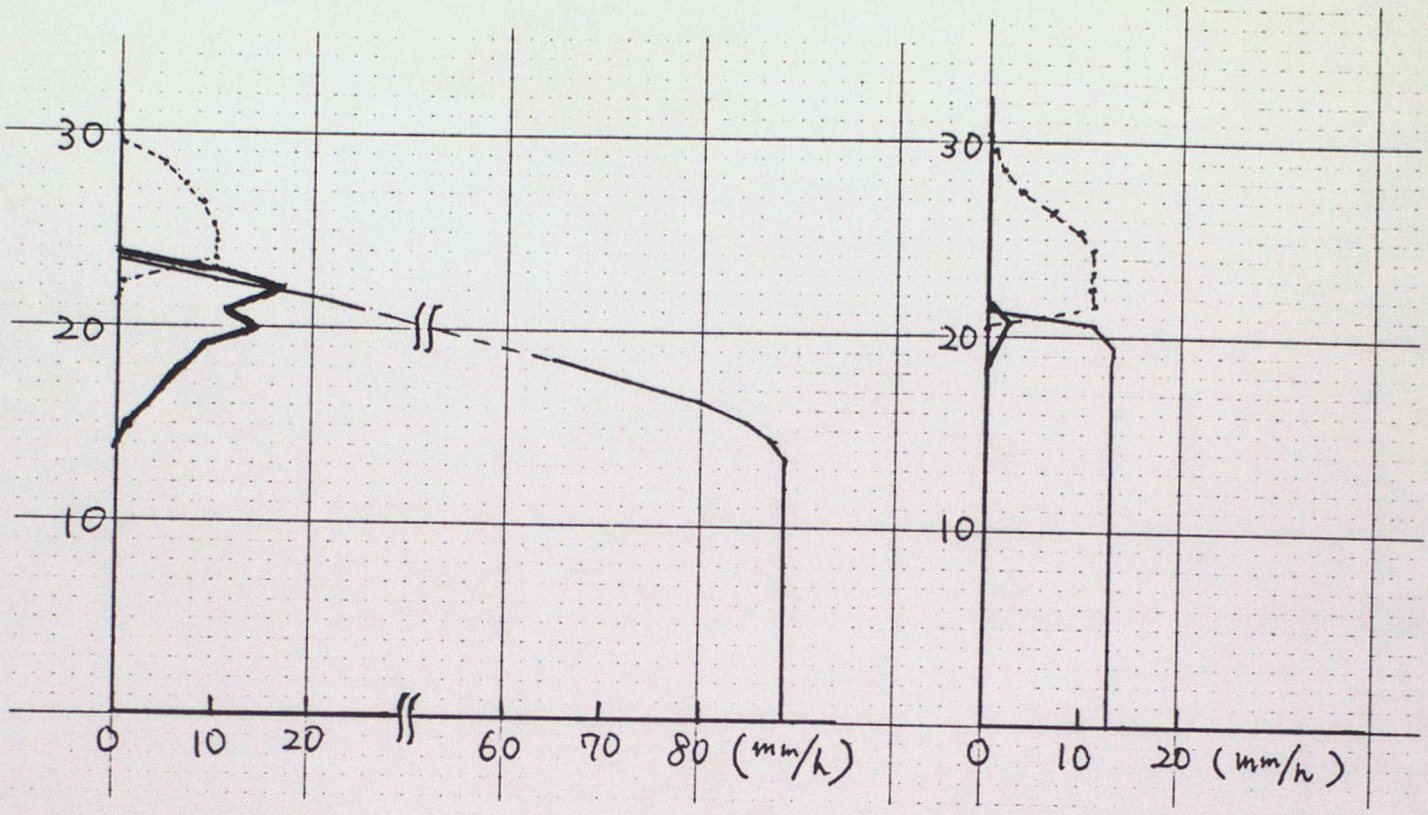

Figure 6 : Vertical distribution of snow rate (dotted line), rainfall rate (thin solid line) and production of rain due to accretion (thick solid line) at the grid point (52,62) denoted by A. The left panel is at timestep 15 and the right one is at timestep 120. The ordinate indicates the model vertical level.

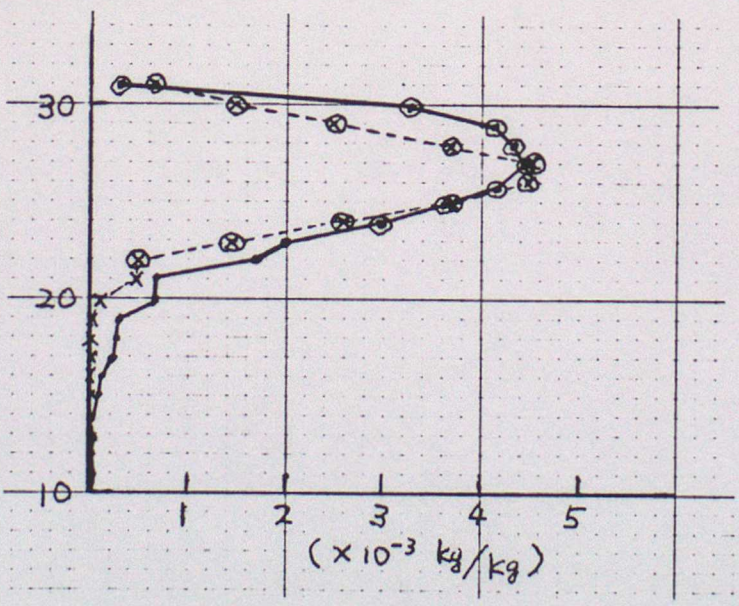

Figure 7 : Vertical profile of liquid water content at the point A at timesteps 15 (solid line) and 120 (broken line). Cloud ice is shown by a circle.

(52,62)

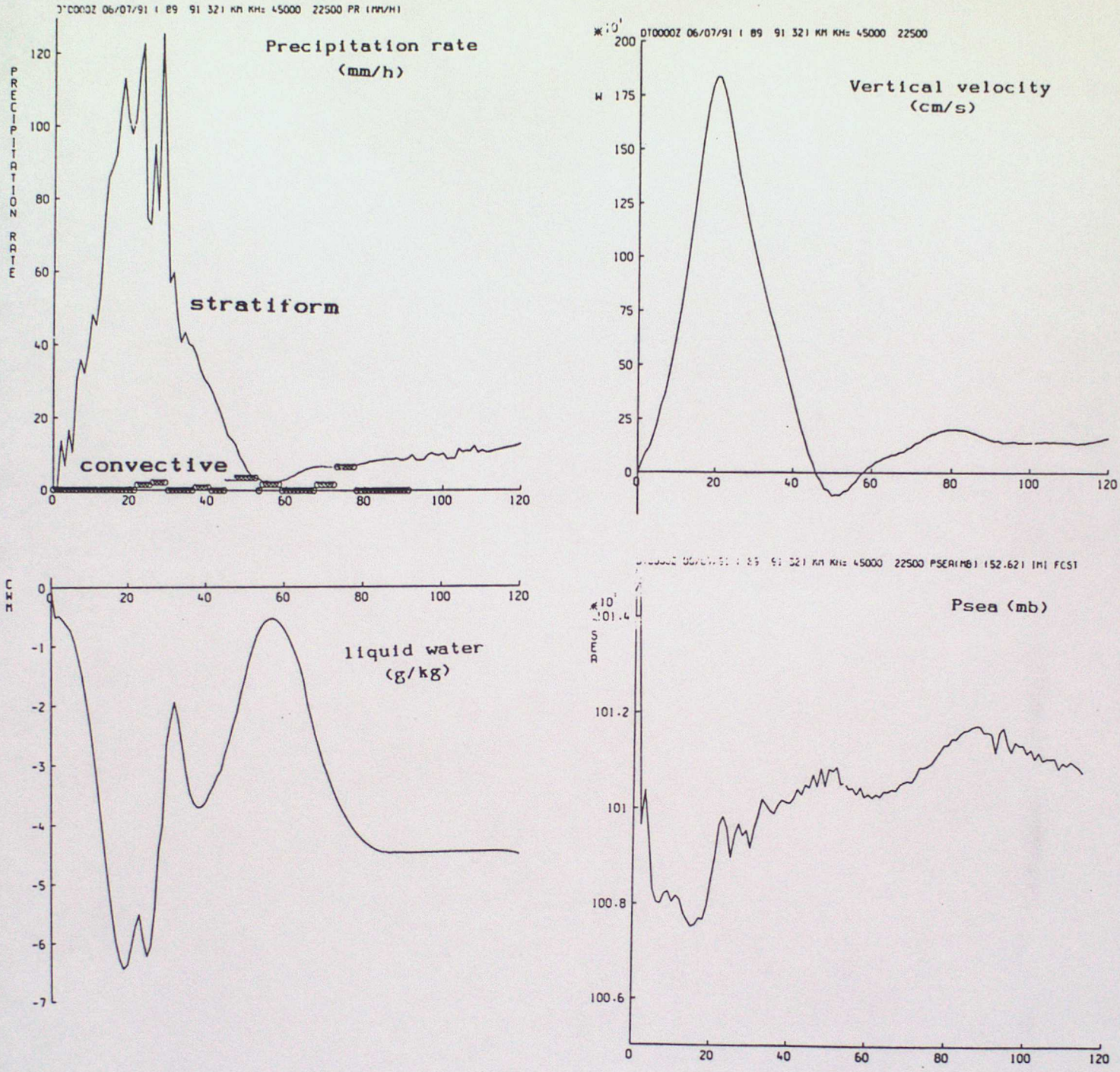

Figure 8 : Time sequence of precipitation rate, vertical velocity, liquid water and sea level pressure at the point A. Abscissa indicates the timestep. Vertical velocity and liquid water are shown at vertical level 27 (about 7700m height).

Figure 9 : Vertical profile of temperature by IMIF at the point A at T+0 and T+1.

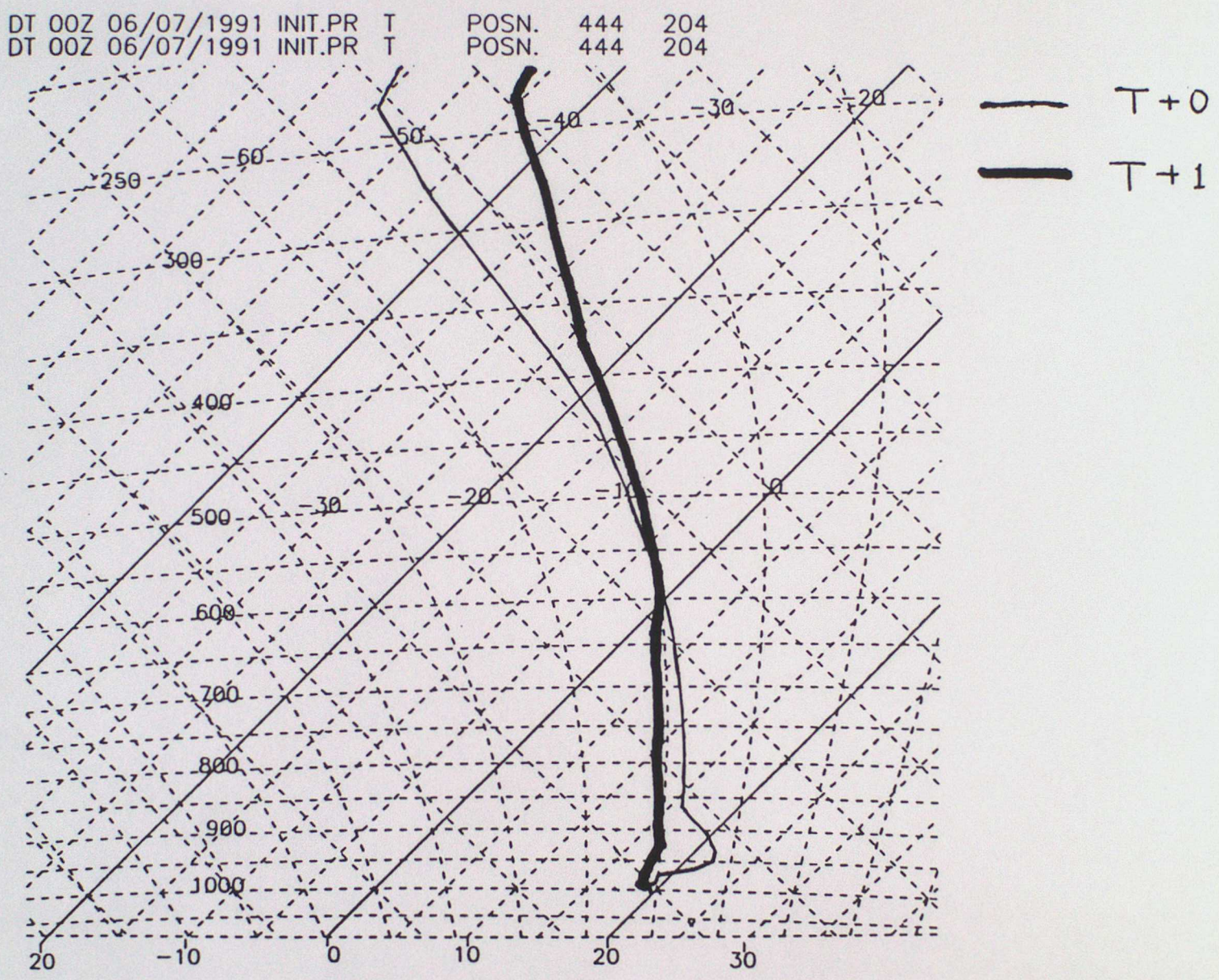

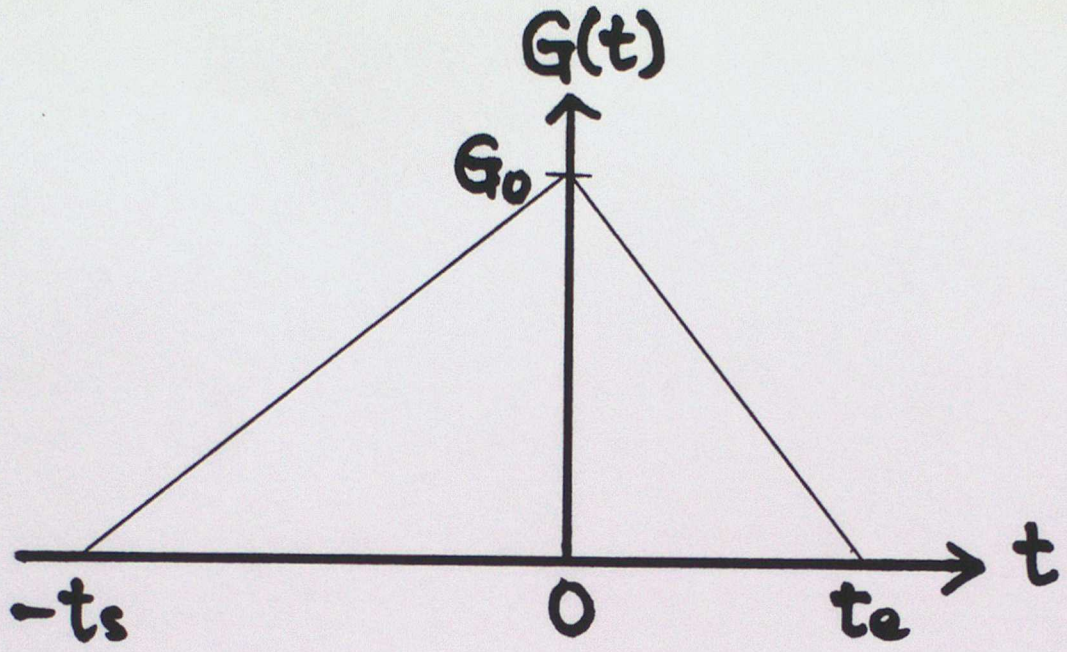

Figure 10 : Nudging coefficient G(t) with respect to time.

Figure 11 : Types of experiments. //// indicates the nudging period towards the IMI analyses.

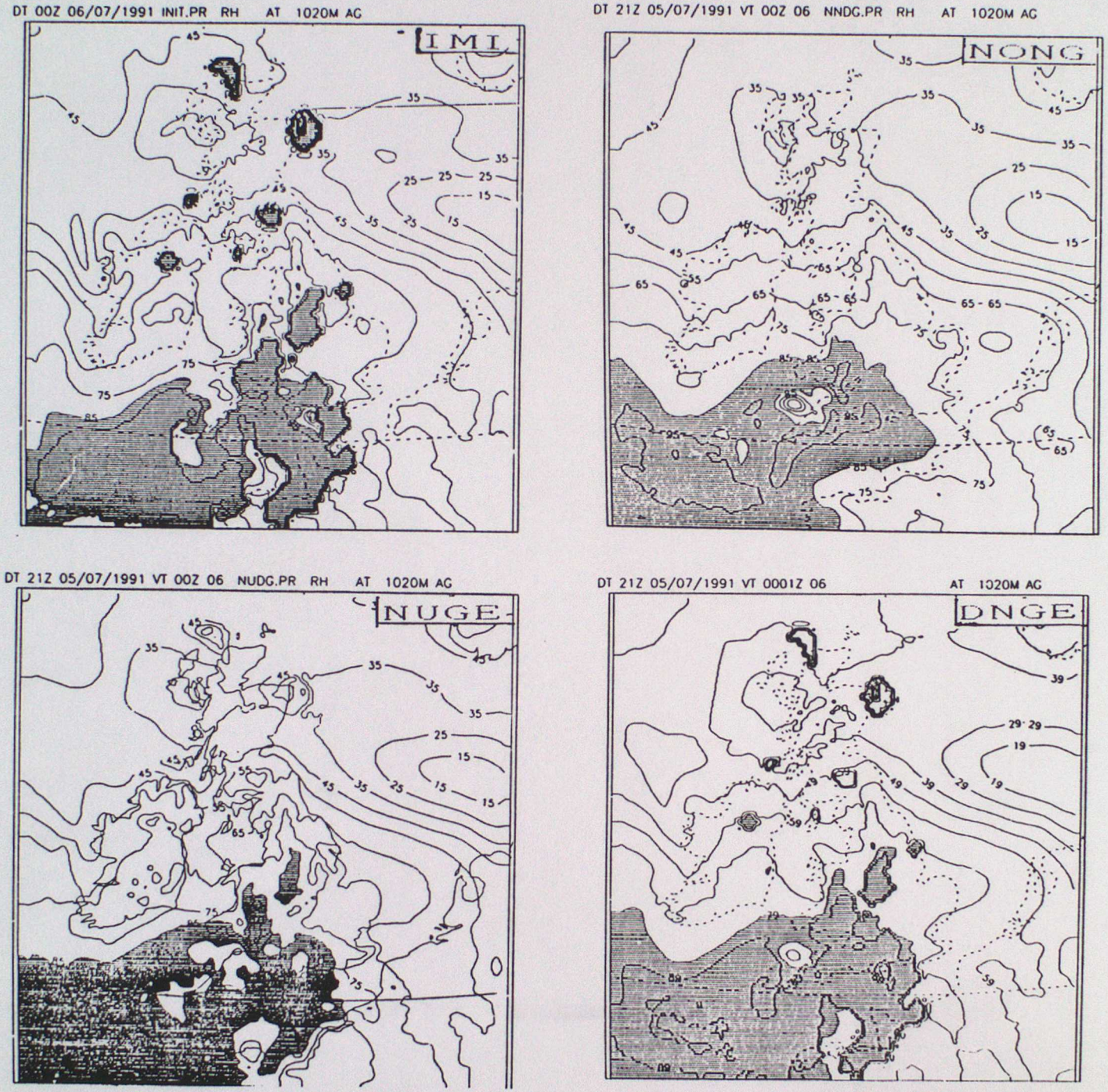

Figure 12 : Relative humidity fields of IMI(analysis), NUGE, NONG and DNGE at T+0 at 1020m height.

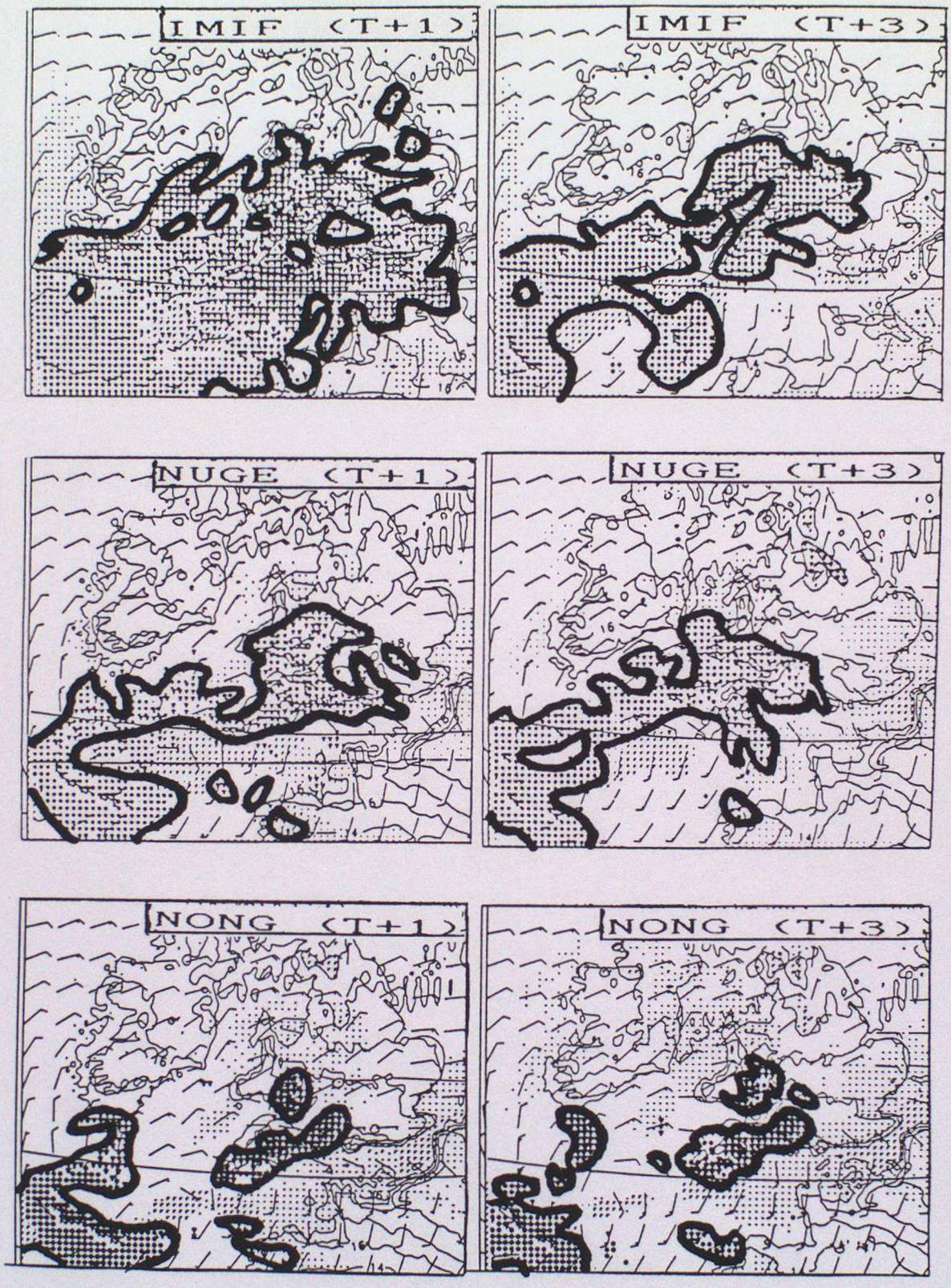

Figure 13 : Present weather of IMIF, NUGE and NONG at T+1 and T+3. Empty and black circles indicate stratiform rain and empty and black triangles show convective rain. Precipitation areas are shown by thick lines. See Figure 18 for details.

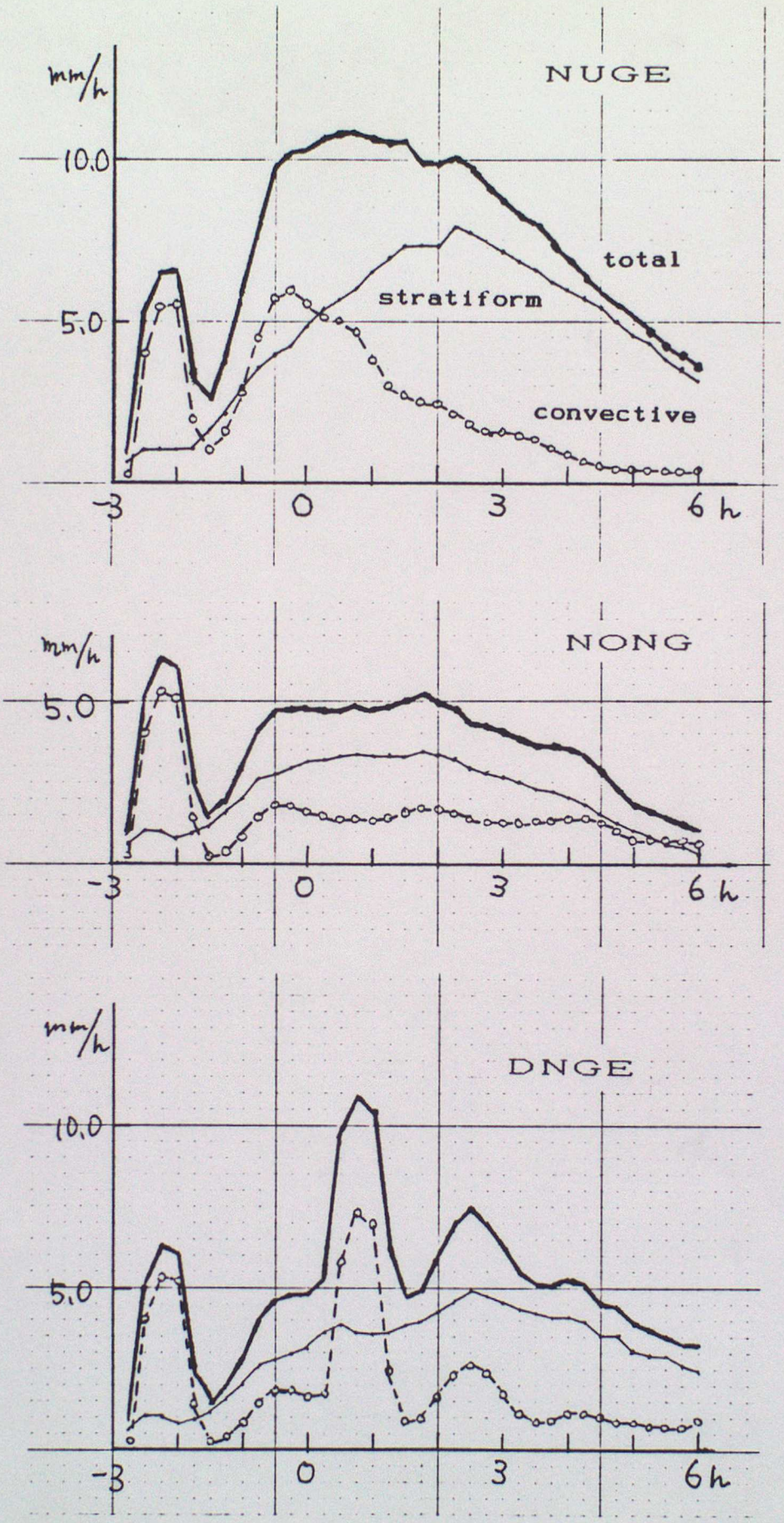

Figure 14 : Same as Figure 2 except for NUGE, NONG and DNGE.

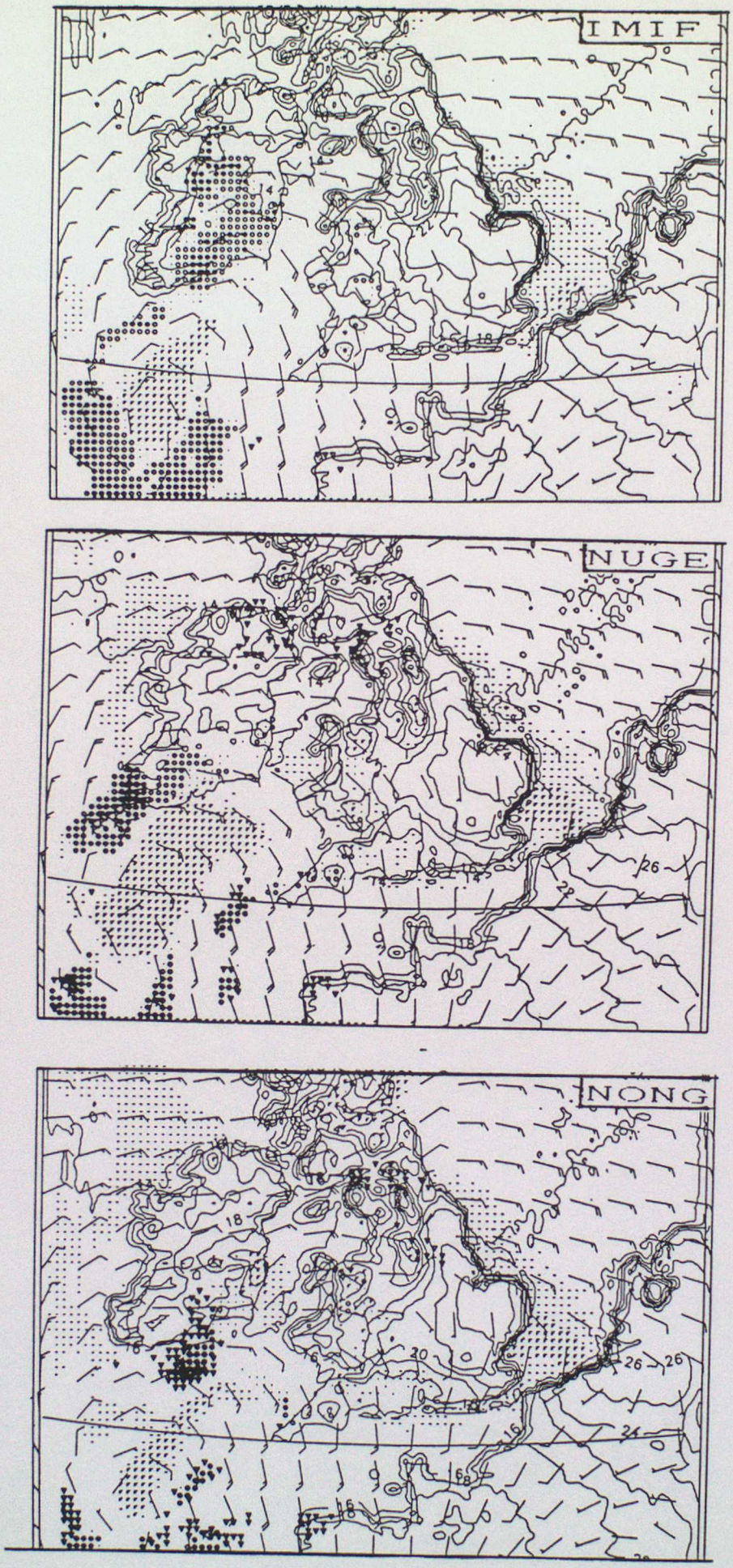

Figure 15 : Forecasts by IMIF, NUGE and NONG at T+9h.

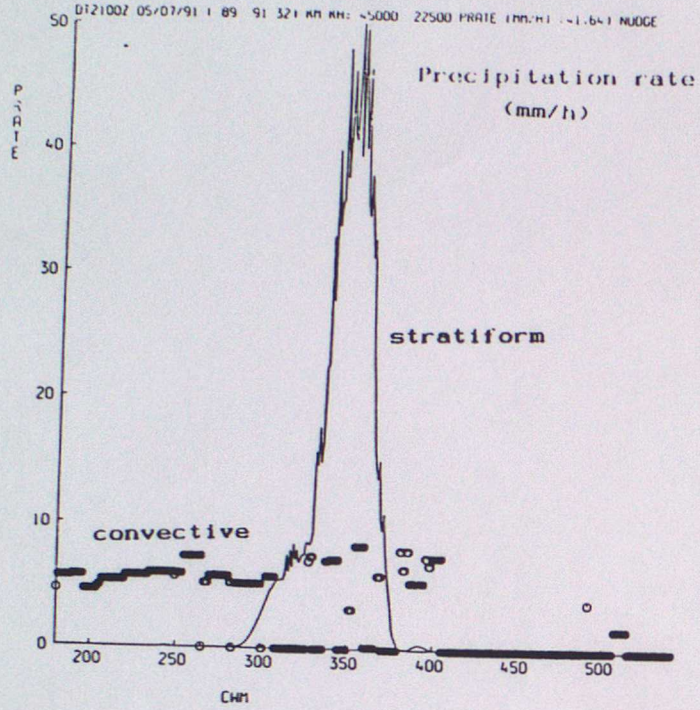

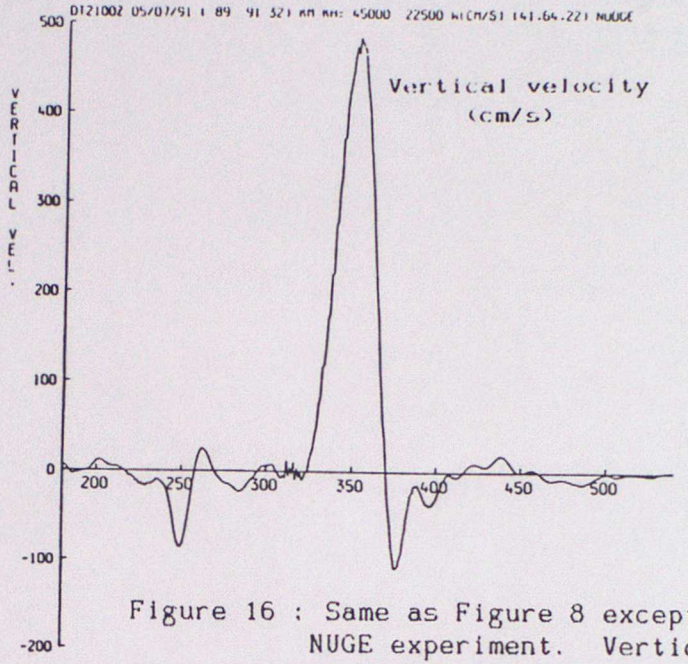

Figure 16 : Same as Figure 8 except for the grid point (41,64) of NUGE experiment. Vertical velocity and liquid water are shown at vertical levels 22 (about 3750m) and 27, respectively.

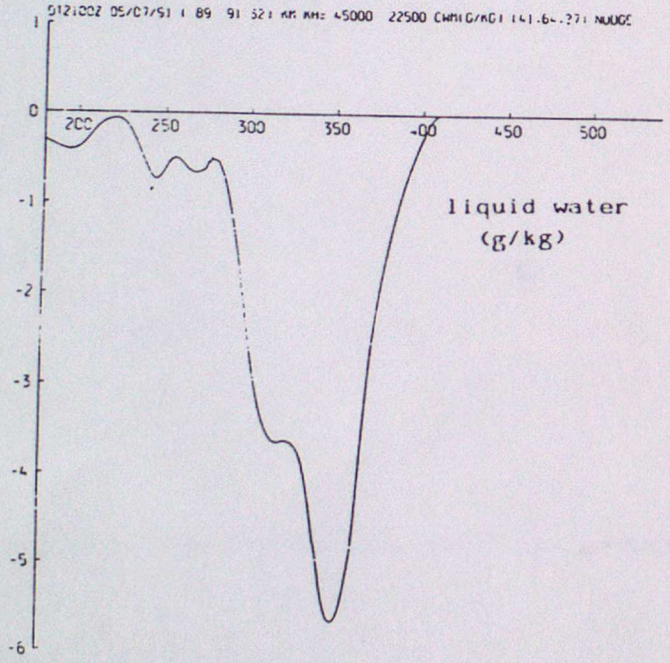

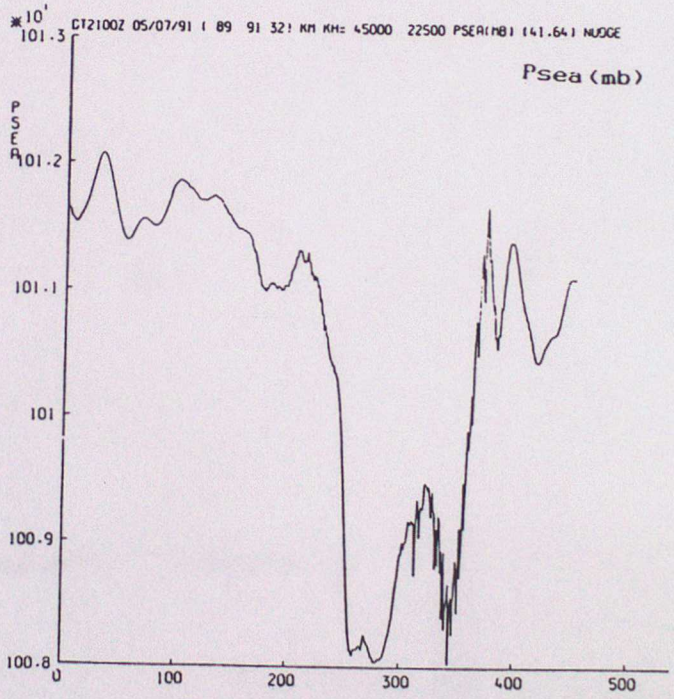

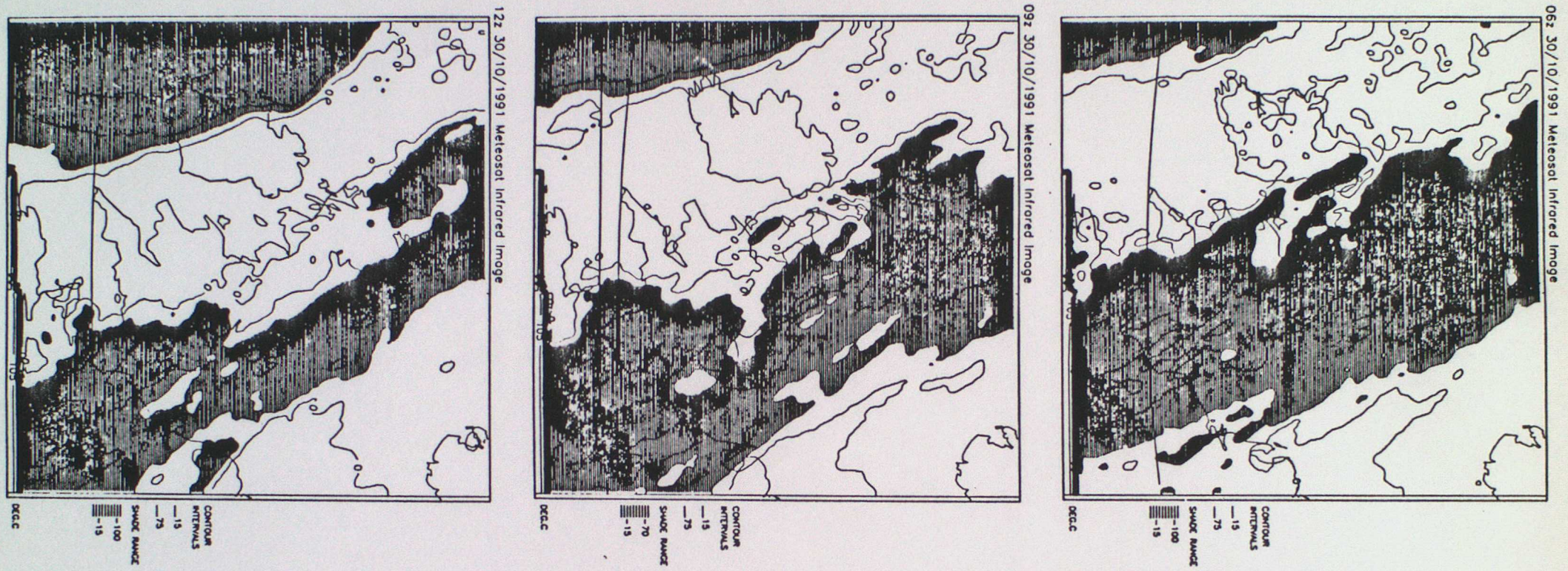

Figure 17 : Meteosat infrared images at 06z, 09z and 12z on October 30th, 1991. The areas with less than -15C temperature are shaded.

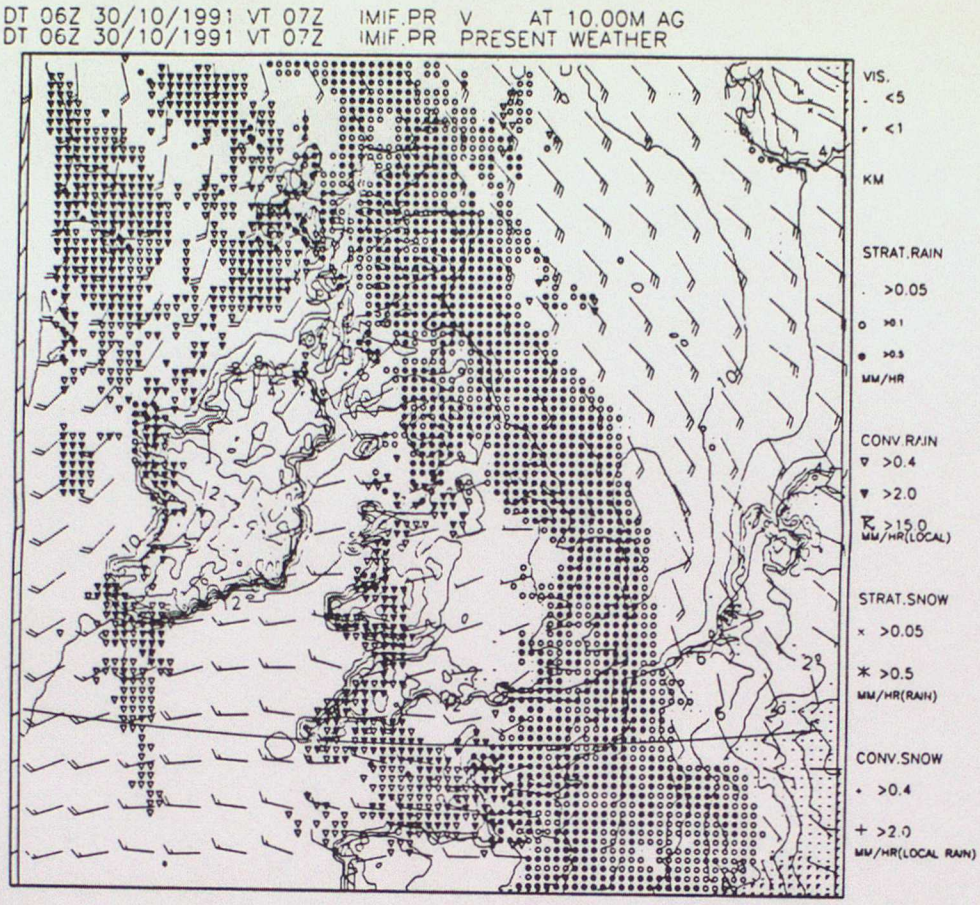

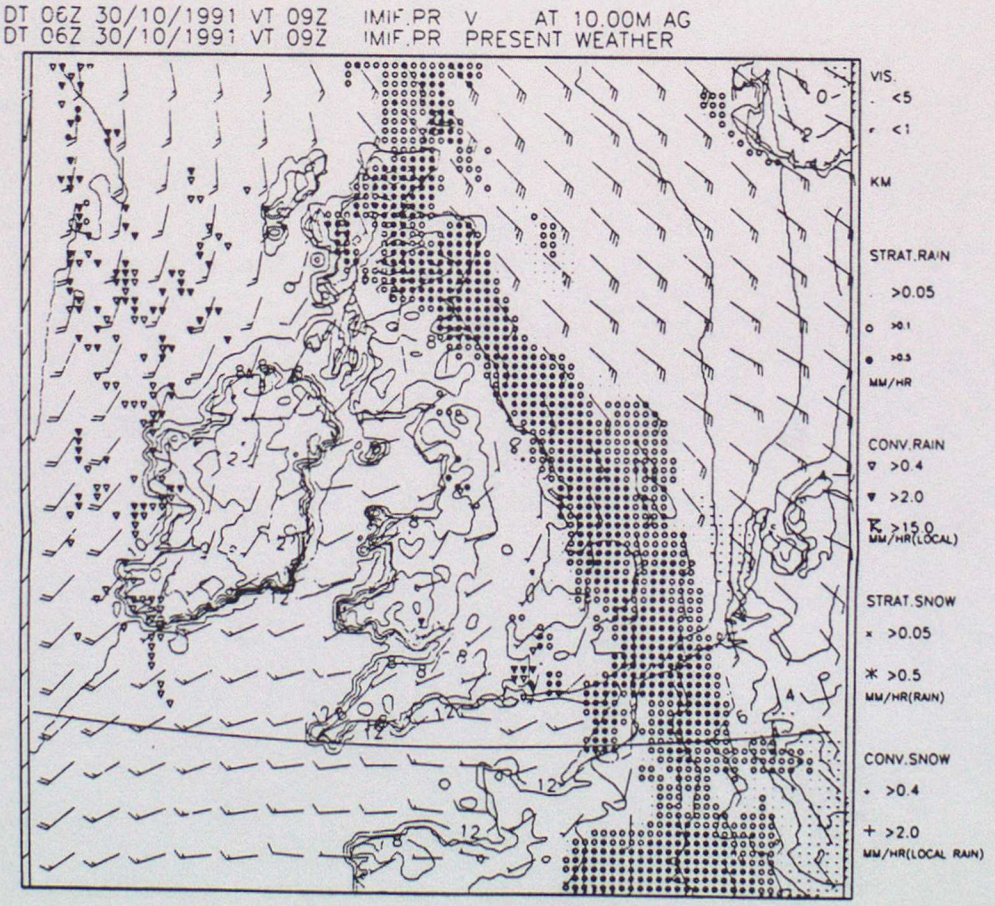

Figure 18 : Present weather of IMIF at T+1 and T+3.

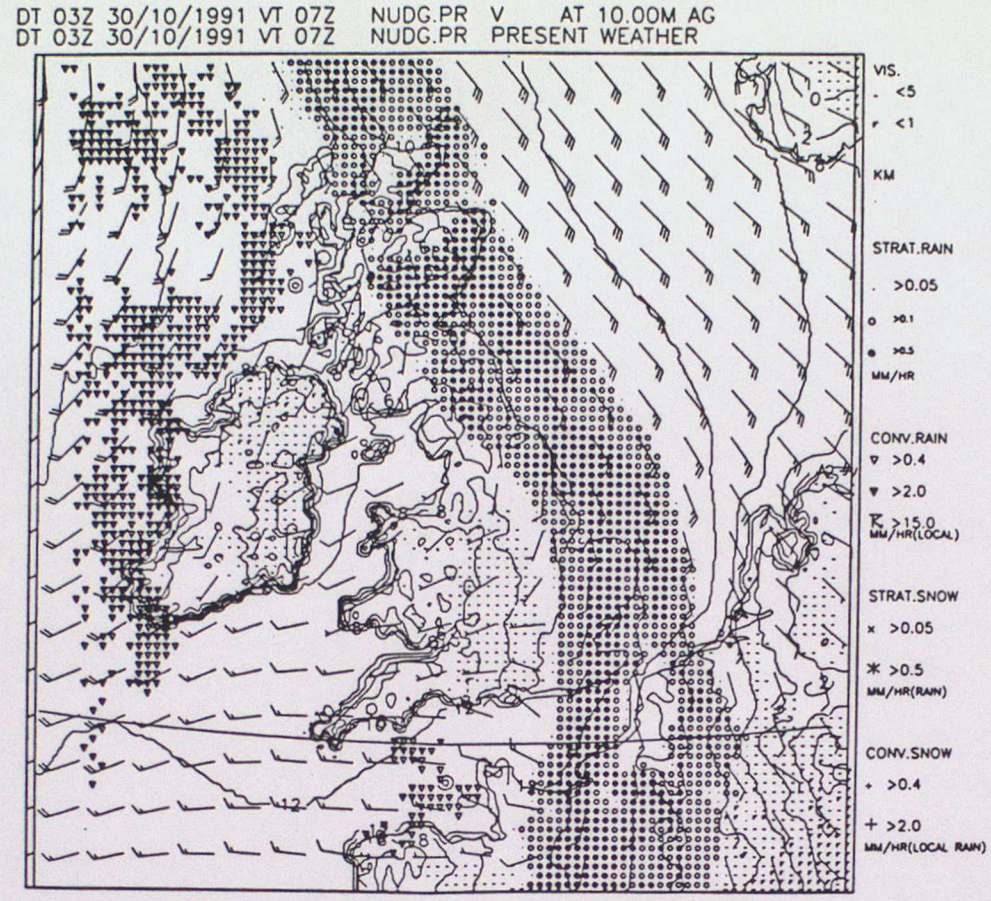

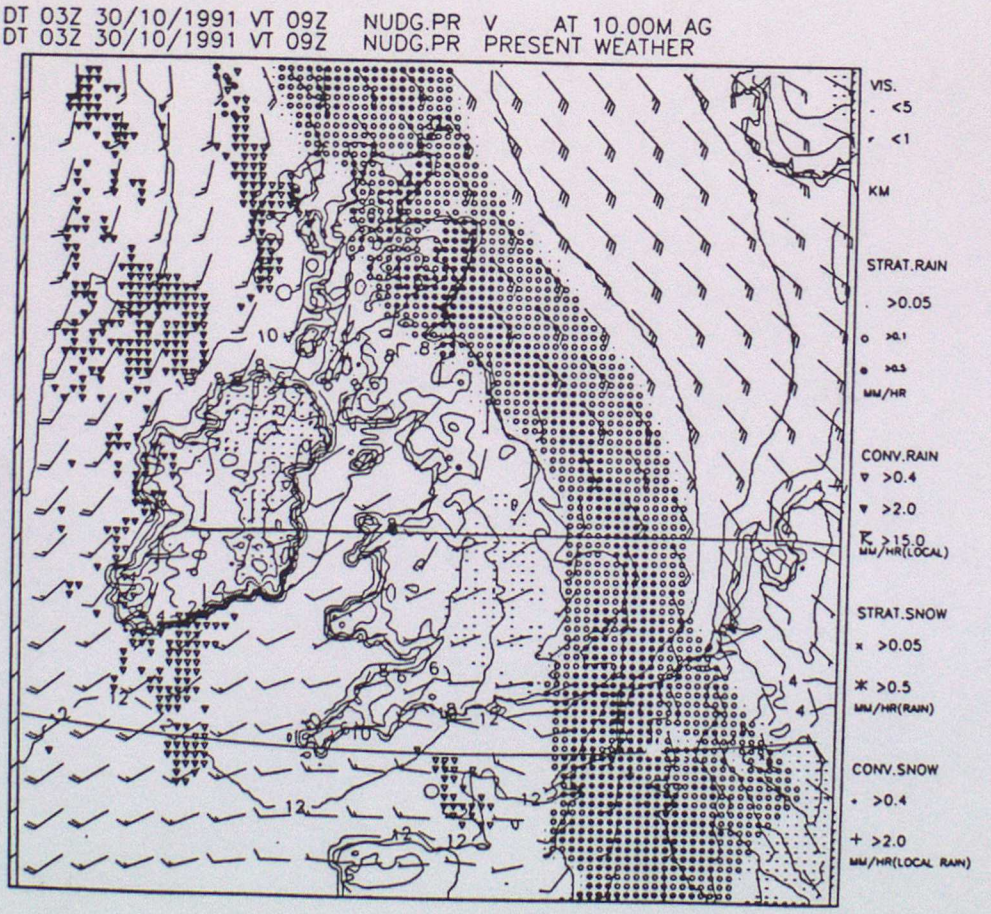

Figure 19 : Same as Figure 18 except for NUGE.

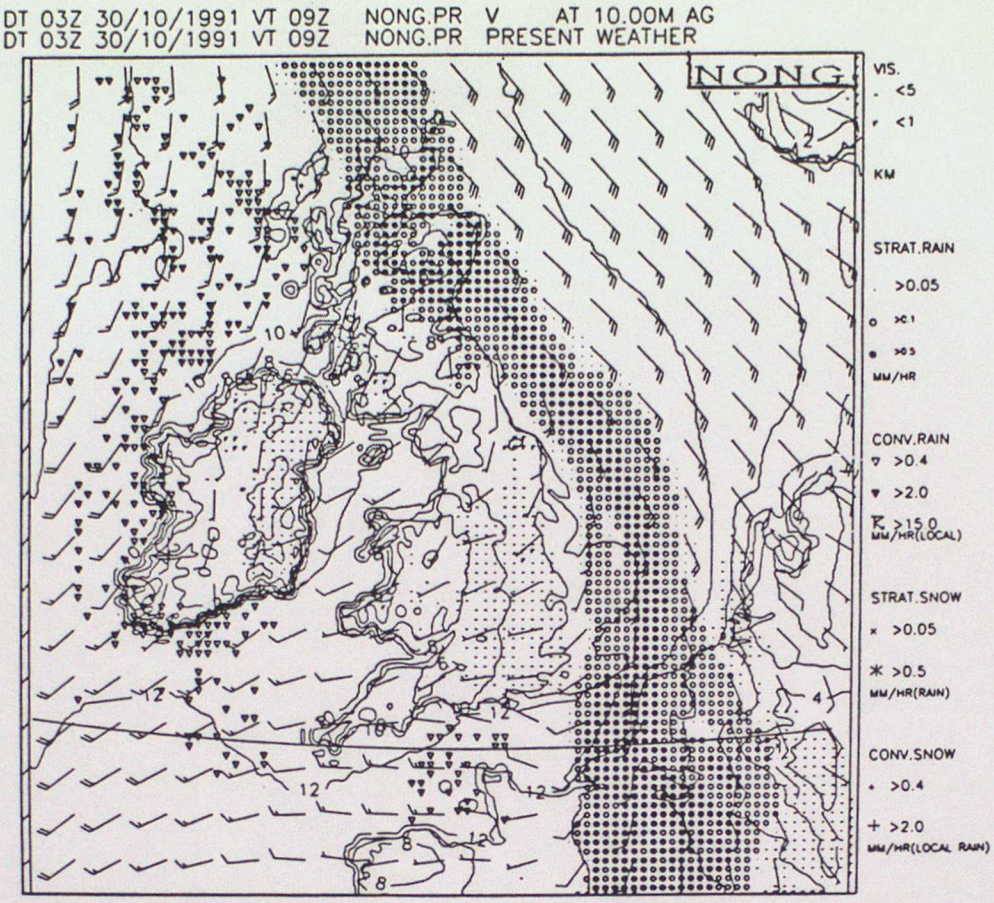

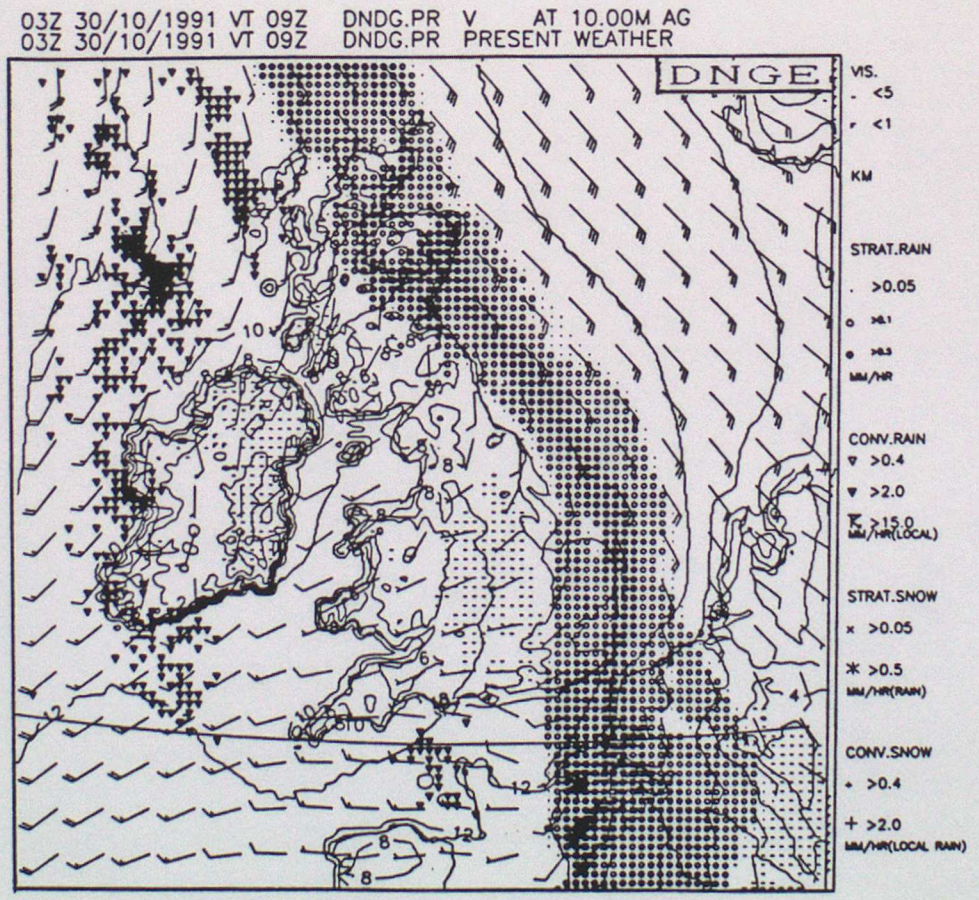

Figure 20 : Present weather of NONG and DNGE at T+3.

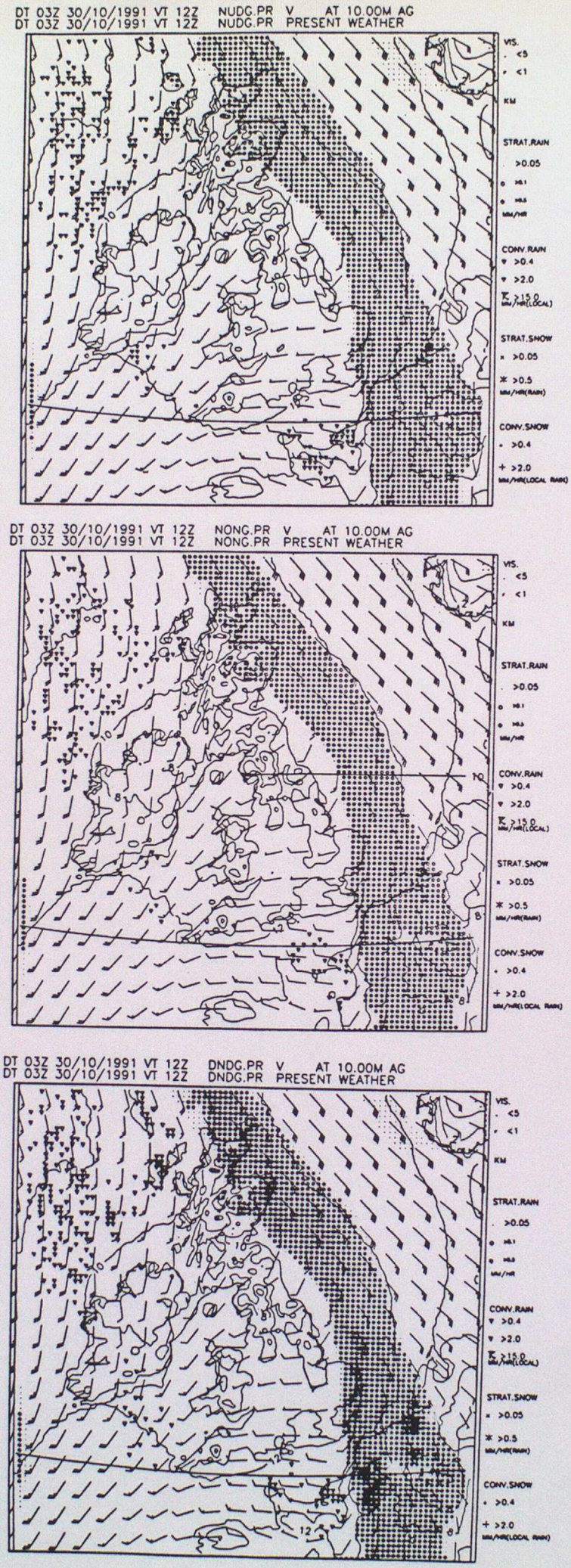

Figure 21 : Present weather of NUGE, NONG and DNGE at T+6.